

Review

The GRB Prompt Emission: An Unsolved Puzzle

Željka Bošnjak ^{1,*},† , Rodolfo Barniol Duran ^{2,*},†  and Asaf Pe'er ^{3,*},† ¹ Faculty of Electrical Engineering and Computing, University of Zagreb, Unska ul. 3, 10000 Zagreb, Croatia² Department of Physics and Astronomy, California State University, Sacramento, 6000 J Street, Sacramento, CA 95819, USA³ Physics Department, Bar Ilan University, Ramat-Gan 52900, Israel

* Correspondence: Zeljka.Bosnjak@fer.hr (Ž.B.); barniolduran@csus.edu (R.B.D.); asaf.peer@biu.ac.il (A.P.)

† These authors contributed equally to this work.

Abstract: The recent multi-messenger and multi-wavelength observations of gamma-ray bursts (GRBs) have encouraged renewed interest in these energetic events. In spite of the substantial amount of data accumulated during the past few decades, the nature of the prompt emission remains an unsolved puzzle. We present an overview of the leading models for their prompt emission phase, focusing on the perspective opened by future missions.

Keywords: gamma-ray burst; prompt emission; relativistic jets

1. Introduction

In the past few years, new observations have led to several breakthroughs in the field of high energy astrophysics. The first detection of the binary neutron star merger event GW170817 by the Laser Interferometer Gravitational-Wave Observatory (LIGO) and the Virgo Consortium coinciding with a short-duration gamma-ray burst (GRB) [1–3] was a watershed moment in astronomy. For the first time, both gravitational waves and electromagnetic waves were detected from the same astrophysical source. Furthermore, this detection firmly placed the merger of neutron star binaries as progenitors of (at least, some) short GRBs. This event was accompanied by a “kilonova”, also robustly establishing neutron star mergers as critical contributors of the production of heavy elements in the Universe [4,5]. These exciting observations have reinvigorated the interest of the astronomical community in understanding the underlying physics of gamma-ray bursts, their associated jets, and progenitors.

A second major breakthrough was the detection of the very high energy (>100 GeV) emission from GRBs by the Major Atmospheric Gamma Imaging Cherenkov (MAGIC) telescopes and High Energy Stereoscopic System (H.E.S.S.) [6,7]. These discoveries provided crucial data for relativistic jets models in which gamma-ray bursts are produced, as well as the nature of high energy radiation processes. On the other hand, neutrinos from GRBs are expected following the interactions of energetic protons that may be accelerated in the GRB environment, however no neutrinos from GRBs have been firmly detected yet [8]. As a result of this lack of detection, one critical piece of information regarding the possible GRB radiation mechanism is still missing. With the advent of new multi-messenger observations, it is becoming increasingly important to revise theoretical models to understand the physics in the vicinity of black holes and neutron stars, the nature of relativistic jets, and the origin of GRBs as the most energetic events in the Universe.

These recent observations add and extend the knowledge gained in the past several decades about the nature of GRBs. Observationally, we know that the vast majority of GRBs have the following common features: (i) Most GRBs consist of highly variable pulses of gamma-ray photons typically lasting dozen of seconds, having a non-thermal spectrum peaking at ~a few 100 keV. (ii) The occurrence rate is approximately once per



Citation: Bošnjak, Ž.; Barniol Duran, R.; Pe'er, A. The GRB Prompt Emission: An Unsolved Puzzle. *Galaxies* **2022**, *10*, 38. <https://doi.org/10.3390/galaxies10020038>

Academic Editors: Elena Moretti and Francesco Longo

Received: 13 December 2021

Accepted: 4 February 2022

Published: 22 February 2022

Publisher's Note: MDPI stays neutral with regard to jurisdictional claims in published maps and institutional affiliations.



Copyright: © 2022 by the authors. Licensee MDPI, Basel, Switzerland. This article is an open access article distributed under the terms and conditions of the Creative Commons Attribution (CC BY) license (<https://creativecommons.org/licenses/by/4.0/>).

day from random directions in the sky [9–11]. (iii) The prompt emission is followed by the afterglow emission detected at lower energies (X-ray, optical, and radio) lasting for days, weeks, months, and (in radio band) years after the main event. (iv) For a number of GRBs, long lasting gamma-ray photons with energy >100 MeV have been observed during the afterglow phase.

The extreme nature of these events—short variability time scales ~ 10 ms, extreme energy of up to (isotropic equivalent) 10^{55} ergs [12], emission over a broad energy scale, from optical to TeV, and the connection of the origin of these explosions with black-hole formation, have posed a challenge for the theoretical modeling of these events. In this review we will focus on the prompt emission of gamma-ray bursts, and provide a short summary of some of the most recent results, and of the proposed models for this emission episode. For more extensive reviews see, e.g., [13–17].

2. Prompt GRB Emission: Key Observational Properties

2.1. Spectral Properties: Sub-MeV Emission

Currently, the wealth of observations on prompt gamma-ray burst emission in the keV/GeV energy range comes from the *Fermi*, *Swift*, *INTEGRAL*, and *Konus-Wind* satellites. The spectrum in sub-MeV energy range is commonly fitted by the so-called Band function [11], which is an empirical function consisting of low- and high-energy power laws, smoothly connected around the peak energy at which most of the energy is emitted. The observed photon spectra indices, α and β of the low- and high-energy power-laws, respectively, may serve to distinguish different radiative mechanisms and properties of the electron distribution (that emit synchrotron radiation, if it is the dominant radiative process, see below). The most recent *Fermi* GBM (Gamma-ray Burst Monitor [18]; covering ~ 8 keV to 40 MeV) gamma-ray burst spectral catalogue [19] provided α values for time-integrated (“fluence”) spectra. When selecting only the models with spectral curvature, the low-energy index values are distributed around $\alpha \sim -1.1$, which is in agreement with previous findings [20,21]. Somewhat steeper low energy spectra $\alpha \sim -0.7$ have been reported for a *Fermi* GBM time-resolved spectral analysis of brightest bursts [22] (excluding the values obtained for simple power-law fits).

Recent works (e.g., [23,24]) provided fits to the gamma-ray burst prompt emission spectra below the spectral peak with not a single, but rather two power laws, connecting at a characteristic low energy spectral break. The break energy below which the spectrum hardened was found to be at (80–280 keV) for a sample of *Fermi* bright long GRBs [24], while it was at lower energies (3–22 keV) for a sample of GRBs contemporaneously observed by *Swift* BAT+XRT [23] (in the latter sample also *Fermi* GBM data were included when available). The importance of these fits lies in the obtained slopes, -0.6 and -1.5 below and above the break, respectively, that are consistent with the prediction of the synchrotron emission theory. A low-energy spectrum having two breaks thus may be a general property of GRB prompt emission though possibly not easily observable with present instruments. On the other hand, studies of the proposed measure of the spectral sharpness, namely the width of the spectral peak [25], showed that a large fraction of the observed GRB prompt spectra is not consistent with the theoretically expected synchrotron model under various assumptions (e.g., delta-function distribution of electrons, and Maxwellian or power-law electron distribution). This result therefore suggests emission mechanisms other than the optically thin synchrotron radiation [26].

A viable alternative is that of a thermal emission, predicted as the first signal arriving from the relativistically expanding fireball, e.g., [27,28]. The thermal spectral component was fitted in the early time-resolved spectra [29,30], or the entire time-integrated spectrum was fitted with a blackbody spectrum [31]. Several authors proposed the fit of a blackbody superimposed on the power-law component in order to fully describe the low energy portion of the spectrum [32–35]. The thermal component exhibited temporal evolution, with a characteristic rise and subsequent decay of the thermal flux. Recent works stress the importance of considering the temporal evolution of the photospheric emission: At

earlier times, $\sim 50\%$ of the analyzed pulses were preferably fit with the photospheric emission [36,37].

High Energy Emission

The first observations of GeV emission from GRBs were obtained by EGRET (the Energetic Gamma-Ray Experiment Telescope, [38]) on board the *Compton Gamma Ray Observatory* in flight 1991–2000 [39,40]. The duration of high energy emission was often longer than the emission at keV, and showed a distinct temporal evolution [41,42].

The *Fermi* LAT instrument (the Large Area Telescope; [43]) is sensitive to γ -rays in the energy range ~ 30 MeV to ≥ 300 GeV. Since its launch in 2008, it asserted several new observational characteristics at energies > 100 MeV [44]: (i) Many of the bright GRBs could not be fitted with commonly used models consisting of the low- and high-energy power law, and an additional power law component was required to fit the high-energy portion of the spectrum and (ii) the emission above 100 MeV tends to be delayed with respect to emission at lower (sub-MeV) energies. When high energy emission was detected, it started during the prompt phase in $> 60\%$ of the cases. Given the *Fermi* LAT field of view, this fraction may be even higher; (iii) the high energy emission lasts systematically longer than the sub-MeV prompt emission, and the high energy flux often follows a power law decay $\sim t^{-1}$. Recently, the two Imaging Atmospheric Cherenkov Telescopes, MAGIC and H.E.S.S. telescopes, reported the observations of the very high energy emission [6,7]. The γ -rays from GRB 190114C were observed in the energy range 0.2–1 TeV starting 57 s after the burst onset. The prompt emission duration of this event was ~ 116 s by *Fermi* GBM and ~ 362 s by *Swift* BAT. The observed very high energy emission was associated with the inverse Compton component in the afterglow phase, however the contribution from the prompt emission at early times could not be excluded [45].

2.2. Light Curve Properties

Prompt GRB light curves show erratic behavior, and so far no common model has been accepted that would fully describe the observed behavior. The duration of emission is associated with the timescale on which the inner engine producing a GRB operates, while the temporal variability reflects its variations in time [46] (though other sources of the observed variability have been proposed, e.g., local relativistic turbulence [47], see below). Broadly, we distinguish two classes of events, short and long GRBs with the dividing line at $T_{90} \sim 2$ s [48], where T_{90} refers to the time in which 5% to 95% of the counts in the 50–300 keV band is accumulated.

It has been recognized that the dividing line of $T_{90} \sim 2$ s depends on the specific gamma-ray detector used, thus additional information must be used to determine if a GRB is “long” or “short” (e.g., [49,50]). This has a theoretical implication: there is strong evidence that “long” GRBs are associated with the collapse of a massive star (the so-called “collapsar” model [51,52]). This evidence is based on the association of long GRBs with core-collapse supernova and thus massive star progenitors [53,54]. Short GRBs, on the other hand, are believed to be associated with the merger of two compact objects [55]. This idea has been proved by the association of the gravitational wave event GW170817 with a GRB (although this GRB may be atypical [1–3]).

In a small number of short GRBs, there is evidence of an extended emission lasting tens of seconds after the short initial spike [56–58], whose origin is still debated. Extended emission from short GRBs was also observed by the *Fermi* LAT at energies > 100 MeV, e.g., in GRB 090510 or GRB 170127C [44].

The observed intrinsic variability during the prompt GRB emission can be rather short, down to \sim tens of millisecond timescale or lower [59,60]. It poses a major constraint on prompt emission models, as the short timescale on which the observed signal can vary in the simplest models is given by $\delta T \sim R / (c\Gamma^2)$ [61] (R is a typical radius of the emitting region and the Γ is the jet bulk Lorentz factor). For GRBs with LAT detection,

short timescale variability during the prompt phase can be found in a handful of bursts, e.g., GRB 131108A [44] and GRB 170214A [62].

2.3. Polarization

The leading models of the non-thermal emission, namely synchrotron emission and Compton scattering, both produce highly polarized emission [63]. However, in order to observe such a polarized signal, one has to break the spherical symmetry, which seems easier during the later time afterglow phase, due to lateral expansion of the slowing-down jet. Indeed, the first claimed detection of polarization signal was during the afterglow phase [64,65]. For a recent comprehensive study of polarization during the prompt phase for different scenarios see, e.g., [66].

High degree of linear polarization was claimed for several bursts, detected by different instruments: RHESSI, BATSE, and Integral [67–72]. Significant linear polarization was detected by the GAP instrument on board IKAROS satellite [73,74] for several GRBs: 100826A ($\Pi = 27 \pm 11\%$), 110301A ($\Pi = 70 \pm 22\%$), and GRB100826A ($\Pi = 84^{+16}_{-28}\%$), in all cases with more than 2.9σ confidence.

In recent years, there have been dedicated missions to study GRB polarization, such as the Indian-led ASTROSAT, which reported several highly polarized signals detected by the CZTI instrument [75–77]. A second dedicated instrument is the POLAR detector [78]. The key result is that, while in many GRBs the time-integrated polarized signal is very low, there are rapid changes in the polarized signal, indicating the need for a time-resolved analysis, in which the signal is much more pronounced.

3. Theories of GRB Prompt Emission

Several current models can successfully interpret some of the spectral and temporal features of GRB emission. The main unknowns in the models for prompt emission are the nature of the energy reservoir and the subsequent energy dissipation, details of the particle acceleration mechanism, and the dominant radiative process. Within current leading models, the observed non-thermal spectrum is interpreted as either [i] a synchrotron and synchrotron self-Compton radiation from a population of relativistic electrons accelerated during the energy dissipation in the outflow (e.g., [79,80]), or [ii] as a Comptonized quasi-thermal emission from the photosphere (e.g., [81–84]). We give an overview and outline the main problems for the several leading models.

3.1. Hot Fireball Model

The hot fireball model assumes the expansion of a fireball composed mostly of photons, electron-positron pairs, and neutrinos [85–87], where magnetic field is energetically subdominant. As the fireball expands adiabatically from a very small radius, the energy of photons and pairs is transferred to protons, which are accelerated to large Lorentz factors [88]. At large distances from the central engine, the kinetic energy of the jet is transformed back to thermal energy, and gamma-rays are produced [89].

Using conservation of energy and entropy, it can be shown (e.g., [15]) that the acceleration of the jet is linear with distance from the base of the fireball R_0 , namely $\Gamma(r) \propto r$. The acceleration proceeds until the outflow reaches the saturation radius $R_s = R_0 \Gamma_s$, where Γ_s is the terminal Lorentz factor. This is true as long as the photons are coupled to electrons in the outflow, therefore, the photospheric radius R_{ph} plays an important role. (i) If $R_s < R_{ph}$, then the jet reaches Γ_s at R_s . (ii) On the other hand, if $R_{ph} < R_s$, then the acceleration mostly stops at R_{ph} [90,91].

The luminosity of the photospheric component in the hot fireball model depends on cases (i) and (ii) mentioned above. For case (i), since the photospheric radius is larger than the saturation radius, the photon temperature decreases due to adiabatic cooling beyond the saturation radius and the thermal luminosity is expected to be lower than in case (ii). The observed photospheric emission is expected to be at a few MeV [85–88]. The emerging spectrum would not be as simple as $f_\nu \propto \nu^2$ below the peak, where ν is the observed

frequency and f_ν is the flux density, however integration from different radii would flatten it slightly to approximately $f_\nu \propto \nu^{1.4-1.5}$ [83,92–94] and an angular dependence of the jet Lorentz factor can flatten it to $\propto \nu^0$ [95], see below. The presence of a strong thermal component in the gamma-ray spectrum would point to the hot fireball model. There is some evidence for a photospheric component in a number of GRB spectra, e.g., [96]. On the other hand, the lack of this clear component has been used to support the magnetically dominated jet model [97], which is described below.

3.2. Particle Acceleration

Following the dissipation of kinetic or magnetic energy, particles are accelerated to high energies. These particles, then, emit the high-energy, non-thermal radiation observed. Modeling this radiation (e.g., as synchrotron emission) provides an indirect evidence for particle acceleration to non-thermal distribution. This was first done in the context of the GRB afterglow [98,99].

The theory of test particle acceleration (i.e., assuming a fixed background) has been well established for many decades [100–105]. In the past 10–15 years, advances in parallel computation, in particular, particle-in-cell (PIC) simulations, have enabled the modeling and studying of this process from first principles [106–109], under various conditions (e.g., magnetization, etc.) [110–113]. There have been several attempts to extend the theory beyond the test particle to include the feedback on the surrounding plasma [114,115]. Alternative theories, such as stochastic turbulence acceleration have also been considered [116].

In recent years, there has been a considerable interest in the theory of magnetized outflows. When the magnetic field is energetically dominant, it may convert its energy to kinetic energy by reconnection of the magnetic field lines, namely, a topological change in the magnetic field structure. Using PIC simulations, many authors have demonstrated that efficient acceleration of particles take place in such reconnection layers [113,117]. Furthermore, the accelerated particles obtain a power law distribution, similar to the expectation from a Fermi-like acceleration [111,113,118–125].

3.3. Internal Shock Model

In the context of GRBs, the first ideas for interpreting the observed highly irregular temporal pattern of radiation came soon after establishing the extragalactic origin of GRBs [10]. It was suggested that energy and matter injection by the compact central object ($<10^7$ cm) does not occur at a steady rate. The resulting outflow would in that case consist of a sequence of “shells” with fluctuating Lorentz factors ([126,127]). In the interaction of a faster shell and a slower one emitted earlier, a shock would develop, which would accelerate electrons to relativistic velocities.

Emission from internal shocks in a relativistic wind with varying Lorentz factors has been studied extensively, e.g., [128–132]. The initial kinetic energy is dissipated in collisions of a series of successive shells emitted from the central engine, having a non-uniform distribution of Lorentz factors $\Gamma(t)$. In the model described by [129], shells interact only by direct collisions, and one shock wave is discretized by the series of shocks (for a comparison with a detailed hydrodynamical calculation, see e.g., [133,134]). The dynamic phase is described by the following parameters: The total duration of the energy ejection by the central engine, the distribution $\Gamma(t)$, and the injected kinetic power during the ejection phase.

For each collision, one can calculate the radius, collision time, Lorentz factor of the shocked material, and the energy dissipated in the collision. The advantage of this model is that the variability time of the energy injection roughly translates into the observed variability time in the GRB lightcurve [135]. The fraction of the thermal energy dissipated in collisions is deposited in electrons in the two colliding shells, while the remaining energy goes into proton acceleration and magnetic field amplification. The efficiency of the energy dissipation process is typically low, $\lesssim 15\%$ [129,136,137], which is the main drawback of the internal shock model.

The microphysics related to a shocked medium is usually parametrized by assuming that a fraction ϵ_e of the dissipated energy is given to the ambient electrons [126,129,131,135]. The electrons are assumed to be accelerated to a power-law, $n(\gamma_e) \propto \gamma_e^{-p}$, above their initial thermal distribution (typical Lorentz factor denoted by γ_m). The slope of the electron distribution p depends on the details of the acceleration process [129]. Under the assumption that the leading radiative process is synchrotron emission from these power-law distributed electrons, the observed high energy photon spectral index β of the “Band”-fitting function, provides the indication for the steepness of the particle distribution, $p \approx 2.5$ [138]. For typical parameters, the synchrotron emission produced by the accelerated electrons in a magnetic field B would occur at observed energy $E_{\text{syn}} = 50(\Gamma_*/300)(B/1000 \text{ G})(\gamma_e/100)^2 \text{ eV}$ [129]. To obtain higher electron Lorentz factors (10^3 – 10^4) in order to reach an observed peak energy at a $\sim \text{few} \times 100 \text{ keV}$, several authors have suggested that only a fraction $\zeta \sim 10^{-3}$ of electrons are accelerated [129,131,139].

Note that there is a large uncertainty in the value of the magnetic field. During the prompt phase, there can be two sources of magnetic field: (i) a strong magnetic field may be associated with the central engine (e.g., [140]). Its strength will decay with distance, however it may still be considerable if the source is highly magnetized, and the dissipation does not occur at too large a distance. (ii) In addition, the magnetic field may be generated at the shock front, obtaining an uncertain fraction (referred to as ϵ_B) of the dissipated energy at the shock.

The accelerated relativistic electrons cool mainly by the synchrotron process, and the associated inverse Compton radiation. The high energy portion of the spectrum is attenuated by photon-photon annihilation, and by the EBL (extragalactic background light) absorption. The low energy portion of the spectrum has a steep cutoff due to self-absorption. The temporal profiles of the prompt emission can be obtained when the contributions from all collisions are taken into account. One example of such study is shown in Figure 1. Here the calculation was performed neglecting the interaction between photons emitted in a shocked region and electrons/photons present in another region (see, e.g., [141]); in addition, the possible contribution of the shock accelerated protons was not considered.

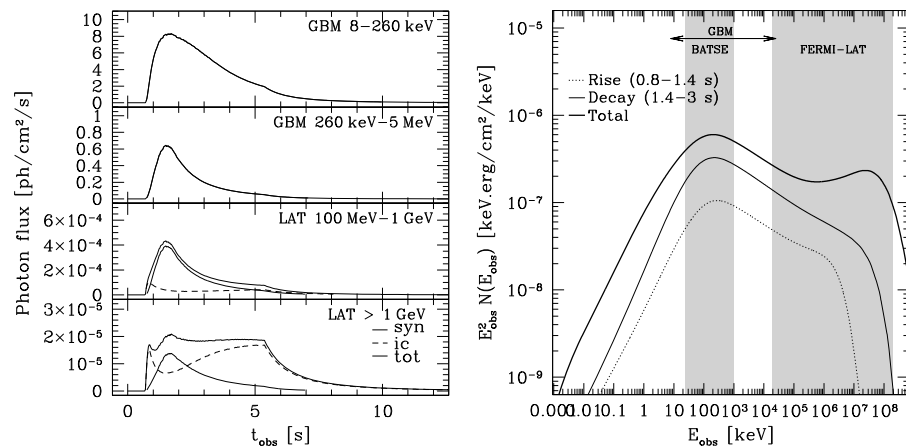


Figure 1. A single pulse burst: the main emission peak is due to the synchrotron radiation. The microphysics parameters used in the simulations are $\epsilon_B = 5 \times 10^{-3}$, $\epsilon_e = 1/3$, $\zeta = 2 \times 10^{-3}$, $p = 2.5$, and $dE/dt = 5 \times 10^{53} \text{ erg s}^{-1}$. As the assumed magnetic field is low, the non-negligible signatures of inverse Compton scatterings are favored in the *Fermi* LAT (the Large Area Telescope) energy range. The process included in calculation are the following: adiabatic cooling, synchrotron emission and synchrotron-self absorption, inverse Compton scatterings, and $\gamma\gamma$ -annihilation. The effects of secondary pairs were not taken into account. *Left*: observed light curves in *Fermi*-GBM (Gamma-ray Burst Monitor and the LAT range). The synchrotron (thin solid line) and inverse Compton (thin dashed line) components are shown. *Right*: observed time-integrated spectrum during the rise, early decay, and whole duration of the pulse. From Credit: [131], reproduced with permission ©ESO [131].

Some authors have pointed out difficulties within the internal shock model when applied to the ‘naked-eye’ burst GRB080319B for which variable prompt optical emission is present [142,143]. The main issue seems to be that the observations point to a very large radius of emission: at these large distances, the gamma-ray flux would be much smaller than observed. These difficulties have served as motivation for alternative models [142].

3.4. The Role of Neutrons in the GRB Jet

It is possible that the GRB jet is also composed of a population of neutrons [144–147]. These neutrons may change the GRB jet dynamics and have an effect on the resulting prompt emission phase [92]. As mentioned before, in the case of the hot fireball model without neutrons, the fireball accelerates as long as the photons are coupled to the electrons. Due to the smaller proton-neutron cross section, when neutrons are present in GRB jet they decouple the protons at a smaller distance from the central engine than the Thomson photosphere. If the decoupling radius is also smaller than the radius R_s where protons attain their maximum speed, then neutrons attain a Lorentz factor $\Gamma_n < \Gamma_s$. This two-fluid state or “compound” state of the jet, similarly to the internal shock model, extracts the kinetic energy of internal motions of the jet. More specifically, it extracts the energy of the streaming of plasma through the neutron component throughout a volume instead of being solely confined to the shock front as in internal shocks [92].

Since this jet is prone to collisions between neutrons and protons, it creates multiple e^\pm pairs, which can have an effect on the emerging gamma-ray spectrum, by cooling via synchrotron and inverse Compton. These cooled pairs form a thermalized pair population which is Coulomb-heated by collisions with protons. This mechanism is able to produce a peak near 1 MeV and a “Band” spectrum with $f_\nu \propto \nu^{1.4}$ and $f_\nu \propto \nu^{-1.5}$ below and above the peak, respectively [92].

Magnetic fields change the spectrum below the peak by significantly cooling the pairs produced in the neutron-proton collisions via the synchrotron process [148]. This does not significantly alter the peak of the spectrum, but does flatten the spectrum below the peak, see Figure 2. It also steepens the spectrum above the peak since inverse Compton emission by pairs becomes less important above the peak in lieu of stronger synchrotron emission below it, which may be in tension with spectral observations [14].

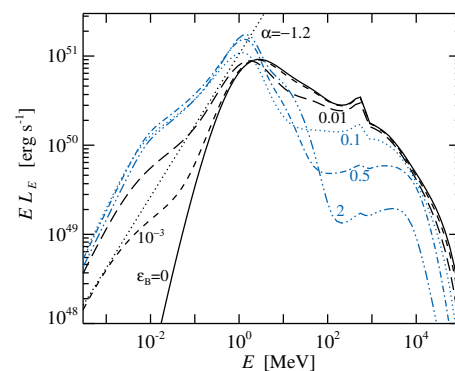


Figure 2. Spectrum of the magnetized, collisionally heated jet. The solid, short-dashed, long-dashed, dotted, dot-dashed, and triple dot-dashed curves correspond to magnetizations of 0, 10^{-3} , 0.01, 0.1, 0.5, and 2, respectively. From ©AAS. Reproduced with permission [148].

3.5. Magnetically Dominated Jet

Some authors have considered models in which the GRB jet is magnetically dominated, that is, where magnetic fields dominate the jet luminosity at the base of the jet [149–152]. In these models, the jet is accelerated as it converts its magnetic energy to bulk kinetic energy. At larger distances from the central engine, the kinetic energy of the jet is transformed to thermal energy, commonly by magnetic reconnection instead of shocks (shocks in this

scenario seems to be too inefficient, e.g., [117,153]), and gamma-rays are produced. For general radiation properties in magnetically-dominated jets, see [154].

Jet acceleration in a magnetic model can occur due to the dissipation of the magnetic field in a striped configuration (such as that of a pulsar wind). This “striped jet” model invokes a magnetized jet with small-scale field reversals or “stripes” [120,155–160], where magnetic reconnection is able to start from small distances and continue as the jet accelerates and collimates. In the case of a black hole central engine, the alternating magnetic fields can be produced by the magneto-rotational instability in the innermost regions of the accretion flow [160]. For the case of a magnetar central engine, the alternating fields can be produced by an oblique dipole rotator [155,156]. Recently, the possibility of a distribution of stripe sizes in a magnetized jet has been considered [160].

In the striped jet, the jet accelerates (as the magnetization drops) up to a saturation radius R_{sat} , where the magnetization reaches ~ 1 . Jet acceleration proceeds, not linearly with the radius as in the hot fireball model, but as $\Gamma(r) \propto r^{1/3}$, e.g., [155,156]. Magnetic reconnection energizes particles and their emission spectrum will depend on the location of the Thomson photosphere compared to R_{sat} . In this model, the observed gamma-ray prompt spectrum can be dominated by a Comptonized thermal spectrum [158,161,162]. Depending on the particle energy injection, the photospheric emission can be subdominant and a non-thermal spectrum can develop. The details of the non-thermal component in this model depend then on the particle energy injection, and several possibilities can be considered [158,163,164].

Jet acceleration can also occur by adiabatic expansion of the outflow [165,166]. In this case, the jet accelerates also as $\Gamma(r) \propto r^{1/3}$ [166]. While there is no magnetic reconnection in this picture, energy dissipation can be driven by internal shocks within the outflow [167,168].

In all models that attempt to explain the prompt gamma-ray emission, reproducing the variability of the observed gamma-ray light curves is crucial. In the case of magnetic reconnection models, including the striped jet model mentioned above, a promising way to explain the light curve variability is to consider small reconnection regions that move relativistically in the co-moving frame of the jet with Lorentz factor $\sim \text{few}–10$ as considered in the “minijets” or “jet in jet” model, relativistic turbulence model, and ICMART (Internal Collision-induced MAgnetic Reconnection and Turbulence) model [47,142,152,169–172]. It is likely that the directions of motion of these small reconnection regions, instead of being isotropically distributed in the comoving frame of the jet, are primarily perpendicular to the direction of the flow [171,172], and this would explain several of the observed prompt GRB temporal and spectral properties [171]. In this particular scenario, the prompt emission would be delayed with respect to the isotropic case, which would allow for the peak of the GRB afterglow to occur during the prompt emission phase in contrast to the simple isotropic model [172], see Figure 3. It would also explain the observed very steep X-ray emission, which is even steeper than the decay expected in the isotropic case [172].

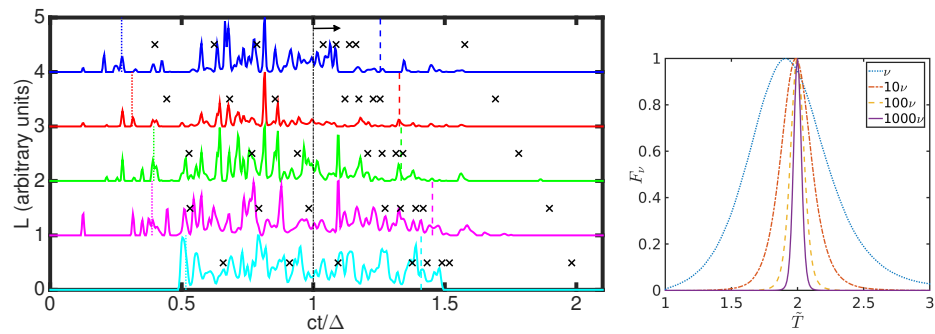


Figure 3. Left: typical prompt emission light curves in the “minijets” model. Degree of anisotropy of minijets’ directions increases from top to bottom. Different light curves (normalized) have been shifted vertically for displaying purposes. Anisotropy shifts the overall light curves to later times. The vertical dotted (dashed) lines for each light curve correspond to the T_{90} duration. We include the observed peaks of the GeV light curves (black crosses) for the sample in [173], scaled for each of the simulated light curves. As the level of anisotropy increases, the peaks of the GeV light curves also shift to later times, making most of them consistent with $t \geq \Delta/c$, where Δ is the shell thickness. In the simplest GRB afterglow model, the deceleration time will occur at times $t \geq \Delta/c$ (see small black arrow) and if the peak of the GeV light curves correspond to the deceleration time, then anisotropic minijets’ directions alleviate the problem of having them at times much less than Δ/c . From [172]. Right: light curves of a single pulse at different frequencies. The pulse clearly becomes narrower with lower frequencies in some magnetic reconnection models as observed in the prompt emission phase. From [171]. Reprinted (and modified) permission of Oxford University Press on behalf of the Royal Astronomical Society.

3.6. Radiative Processes

3.6.1. Synchrotron Emission and Inverse Compton Scatterings

Among the non-thermal radiative processes, synchrotron emission from relativistic electrons has been considered an important mechanism in the context of the prompt emission of GRBs [79,135,174–176]. Several authors have taken a general approach and determined the source properties (e.g., jet bulk Lorentz factor, electrons’ Lorentz factor, distance from the central engine to location where gamma-ray are produced) by assuming that the peak of the gamma-ray emission spectrum is produced by the synchrotron process (e.g., [31,130,132,177]; for the case of a magnetic jet, see, e.g., [178]). The major challenge for the synchrotron model is posed by the observed hard low energy spectrum that is in apparent contradiction with the predictions of the simple synchrotron model (e.g., [99,138,179]). The flux $f_\nu \propto \nu^{-1/2}$ below the peak of the spectrum is expected when electron’s radiative time scales are much shorter than the dynamical times (‘fast-cooling regime’) [99]. We define γ_c as the Lorentz factor of electrons whose synchrotron loss timescale is equal to the adiabatic cooling timescale t_{ex} , $\gamma_c = 6\pi m_e c / (\sigma_T B^2 t_{\text{ex}})$, where m_e is the electron’s mass, c is the speed of light, and σ_T is the Thomson cross-section. The synchrotron fast-cooling regime is then characterized by $\gamma_c < \gamma_m$. This regime is favorable for prompt gamma-ray emission as it has a high radiative efficiency. There have been several studies reconciling the observed spectrum with the synchrotron emission, and proposing solutions for harder spectral slope: The pitch-angle distribution [138], the small scale structure of the magnetic field [180,181], or processes that involve the appearance of a quasi-thermal component in addition to non-thermal synchrotron [27,182].

It is also possible to have the synchrotron mechanism responsible for the GRB prompt phase, however modified by including an additional source of cooling due to inverse Compton scatterings [183–186]. The soft low-energy spectral slope of the photon spectrum $\alpha = -1.5$, resulting from the assumption of fast cooling synchrotron spectrum, could be hardened if a sub-dominant radiative process (like inverse Compton scatterings) transferred around 20–40% of the energy from the synchrotron component to higher energies [185]. There are two parameters that control the importance of inverse Compton scatterings:

$w_m = \gamma_m \epsilon_m$, where $\epsilon_m = h\nu_m/m_e c^2$ and $\nu_m = \nu(\gamma_m)$, determine whether the scatterings occur in the Thomson regime ($w_m \ll 1$) or if Klein–Nishina effects need to be taken into account; another parameter is Y_{Th} , which determines the intensity of the inverse Compton component peaking at high energies. When Klein–Nishina corrections are important ($w_m \gtrsim 1$), the cross section and the energy boost are reduced so that the ratio of the total energy in the inverse Compton component over the total energy in the synchrotron component becomes $E_{\text{ic}}/E_{\text{syn}} \ll Y_{\text{Th}}$ [131]. It has been shown that the physical conditions in the emitting region allow for a synchrotron component peak at \sim a few 100 keV, and a moderately efficient inverse Compton scatterings in the Klein–Nishina regime. In particular, in the internal shock scenario [185], a large fraction of the dissipated energy $\epsilon_e \sim 0.1$ – $1/3$ should be injected in a small fraction of electrons $\zeta \lesssim 0.01$ and the fraction of the energy injected in the magnetic field should remain low, $\epsilon_B \lesssim 10^{-3}$. Additionally, the ‘marginally fast cooling regime’ was proposed by [185], considering that electrons are in the fast cooling regime but not deeply in this regime (i.e., $\gamma_c \lesssim \gamma_m$ rather than $\gamma_c \ll \gamma_m$). When the cooling frequency becomes close to the frequency ν_m , the observed photon index can become very close to the value $-2/3$ below the cooling frequency, even in the fast cooling regime. This solution requires collisions at small radii and/or low magnetic fields. However, in this context, and focusing on conditions where synchrotron cooling is balanced by a continuous source of heating, one naturally finds solutions consistent with those of the minijets model in the magnetically dominated jet described above [187], where dissipation occurs far from the central engine.

High energy gamma-rays in the prompt GRB phase could be also produced by inverse Compton scattering of synchrotron photons: “synchrotron-self-Compton” SSC emission. However, in its simplest form, this mechanism either produces a more energetic component in very high energy gamma-rays or would require a more energetic component as a low-energy synchrotron seed, which is inconsistent with observations [143,188]. On the other hand, the SSC it is defined in the beginning of the paragraph origin of GRB prompt emission seems to work well in the context of the relativistic turbulence model [142].

3.6.2. Comptonized Thermal Radiation

Photospheric (thermal) emission is inherent to the “fireball” model as, following the initial explosion, the plasma is optically thick, and photons cannot escape. Rather, they are coupled to the expanding gas, converting their internal energy to kinetic energy of the expanding gas. Only when the gas sufficiently expands does the optical depth decrease such that the photons escape. It is therefore of no surprise that the very first cosmological GRB models considered photospheric emission as a leading radiative process [81,86,87,189]. However, the fact that the prompt spectra appears non-thermal has led to focus on other broad-band models, in particular synchrotron.

Renewed interest in this model resumed in the early 2000s, with the realization that the synchrotron model appears too broad to explain the steep low energy spectral slope (the ‘synchrotron line of death’) [190]. Several authors considered a possible contribution from photospheric photons to the observed spectra [27,82,90,91,191,192]. It was realized that the observed spectrum of photons originating from the photosphere did not necessarily resemble a “Planck” function, due to two complementary effects. The first is possibly sub-photospheric energy dissipation, e.g., by lateral shock waves at the boundary between the relativistic jet and collapsing star, or reconnection of magnetic field lines, which heats the electrons in the plasma [158,161,193,194]. The dissipation heats the electrons, which then serve as seeds for inverse-Compton scattering. When such events occur below the photosphere, the original ‘Planck’ spectrum can be heavily modified, and the result depends on the details of the energy exchange between the particles and photon fields; this is demonstrated in Figure 4.

A second, independent effect is the aberration of light, which is essentially the relativistic version of the well-known limb darkening effect from solar observations. Due to the probabilistic nature of the scattering process, the photosphere is in fact ‘vague’, namely

the last scattering location of photons can occur in various spatial locations (as opposed to a single surface) [83,92,93,95,195,196]. This location is angle-dependent: at high angles, it occurs, on the average, at larger radii than at angles $< 1/\Gamma$ (the jet Lorentz factor). In a spherical explosion, this aberration leads to a modification (mainly) of the Rayleigh–Jeans part of the spectrum. However, the jets are not spherical, but have some lateral shape (angle-dependent Lorentz factor). In this case this effect becomes very pronounced and affects both the low as well as the high energy spectral slopes making both of them shallower than the naively expected Rayleigh–Jeans shape [95,197,198], although steeper than the expected from synchrotron radiation, making the spectral slopes consistent with the data [36,164,199,200].

An interesting version of the photospheric model is the ‘back scattering’ dominated model [201,202]. In this model, the jet drills a funnel through the stellar envelope, and accelerates a ‘cork’ made of stellar material ahead of it. The photons originate from e^\pm pair annihilation close to the central engine, across the virtually empty jet before being back-scattered from the cork material ahead of them (if the cork does not disintegrate too rapidly). Although in the cork frame they are scattered backward, they will be detected by an observer located off axis, due to the relativistic angle change between the cork and observer’s frame. It was recently demonstrated [203,204] that the resulting spectra in this setup is in excellent agreement with the observed, both at low and high energy. Furthermore, this model naturally explained the observed peak energy—total energy relation (known as “Amati” correlation; [205]) without the need to invoke any additional assumption.

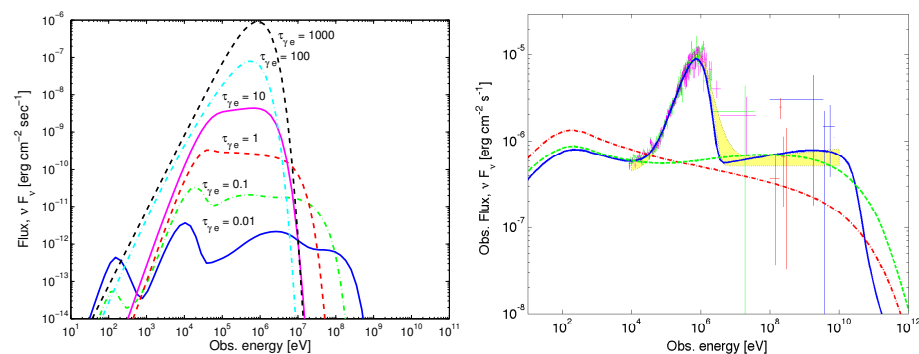


Figure 4. Left: time averaged broadband spectra expected following kinetic energy dissipation at various optical depths. For low optical depth, the two low energy bumps are due to synchrotron emission and the original thermal component, and the high energy bumps are due to inverse Compton. At high optical depth, $\tau \geq 100$, a Wien peak is formed at 10 keV and is blue-shifted to the MeV range by the bulk Lorentz factor of ~ 100 expected in GRBs. In the intermediate regime, $0.1 \lesssim \tau \lesssim 100$, a flat energy spectrum above the thermal peak is obtained by multiple Compton scatterings. Figure taken from [194]. ©AAS. Reproduced with permission. Right: spectral decomposition of GRB 090902B (taken 9.6–13.0 s after the GBM trigger) enables clear identification of the physical origin of the emission. The dash-dotted (red) curve shows the spectrum that would have been obtained if synchrotron radiation was the only source of emission. The dashed (green) curve shows the resulting spectrum from synchrotron and synchrotron self-Compton SSC, and the solid (blue) curve shows the spectrum with the full radiative ingredients (synchrotron, SSC, the MeV thermal peak, and Comptonization of the thermal photons). From [206]. Reprinted (and modified) permission of Oxford University Press on behalf of the Royal Astronomical Society.

3.6.3. Hadronic Processes

Hadronic processes refer to radiation from protons that are present in the GRB outflow [207–214]. These protons could in principle radiate via the proton synchrotron process and produce the observed gamma-ray prompt emission. However, even if these protons do not produce the observed gamma-ray spectrum, if present, they could potentially interact with photons and decay to pions through the delta resonance: photopion

processes (see, e.g., [207]). Pions decay into neutrinos, making GRBs possible sources of neutrinos; into leptons, which could in turn undergo synchrotron emission, and neutral pions decay directly to two high energy photons. Proton-photon interactions can also generate electron-positron pairs directly via the Bethe–Heitler process. Several authors have used the observed 100 MeV LAT prompt emission to constrain hadronic models [209–211,213]. To explain the 100 MeV LAT photons during the prompt phase, (i) the photopion and Bethe–Heitler processes require energy in protons larger than the observed gamma-ray energy by a factor of a thousand or more and (ii) the proton synchrotron mechanism requires protons to have a minimum Lorentz factor of $\sim 10^6$, which is much larger than expected if the protons are accelerated in shocks [213]. This makes hadronic processes less energetically viable than leptonic models.

4. Discussion: A Look into the Future

With the advent of observations at very high (GeV/TeV) energies by *Imaging Atmospheric Cherenkov Telescopes* such as MAGIC [6] and H.E.S.S. [7], and the perspective being opened by the future multi-messenger environment for gamma-ray bursts, the premise of radiation models will inevitably be revisited. At very high energies, the future Cherenkov Telescope Array (CTA) will provide improved sensitivity to up to an order of magnitude with respect to current IACTs [215,216]. Although the recently provided detection rate is modest (during the prompt phase, it is expected to be $\lesssim 1$ per year [217,218]), if CTA provides GRB observations with high photon statistics, it will help constrain emission models (e.g., the properties in the emission site of high-energy photons). The observed variability could help differentiate between emission mechanisms [217]. As the *Fermi* LAT spectra often displays a hard power-law spectrum extending to GeV energies, the observations of the high energy part could provide the information on the total radiated energy, and the bulk Lorentz factor can be constrained if the high-energy spectral cutoff due to pair production is identified [217]. At the low energy end, the *SVOM* (Space-based multi-band astronomical Variable Objects Monitor) mission aims to survey the high-energy sky and follow-up transients at optical and X-ray wavelengths [219]. Its main goals are observations of the high-redshift GRBs ($z > 5$), and faint/soft nearby events. It will also likely be the alert facility for CTA, opening e.g., the possibility of detecting low luminosity events which are not triggered by the current missions [220]. Other future multi-messenger facilities for GRB-related science include, e.g., the third-generation gravitational-wave observatory Einstein Telescope [221], the development of the extension of the IceCube Neutrino Observatory IceCube-Gen2 [222], and ATHENA [223] satellite for the X-ray domain. Upper limit of neutrino flux from GRBs [224] as well as the observations at longer wavelengths (e.g., using the upcoming Vera Rubin Observatory or the Square Kilometer Array-SKA) could provide information on jet composition—baryonic or magnetic jet. The observational advances need however to be followed by theoretical effort, i.e., numerical simulations of the processes involved in the production of prompt emission, such as energy dissipation and particle acceleration, in order to fully understand the extreme conditions in which gamma-ray bursts are produced.

Author Contributions: All authors Ž.B., R.B.D. and A.P. have contributed to writing—review and editing. All authors have read and agreed to the published version of the manuscript.

Funding: R.B.D. acknowledges support from the National Science Foundation under grants 1816694 and 2107932. A.P. was partially supported by the EU via the ERC consolidating grant 773062 (O.M.J.). Ž.B. acknowledges support from the Croatian Science Foundation (HrZZ) Project IP-2016-06-9782.

Institutional Review Board Statement: Not applicable.

Informed Consent Statement: Not applicable.

Data Availability Statement: Not applicable

Acknowledgments: We thank P. Beniamini, D. Giannios and P. Kumar for useful discussions related to this manuscript.

Conflicts of Interest: The authors declare no conflict of interest.

References

- Abbott, B.P.; Abbott, R.; Abbott, T.D.; Acernese, F.; Ackley, K.; Adams, C.; Adams, T.; Addesso, P.; Adhikari, R.X.; Adya, V.B.; et al. GW170817: Observation of Gravitational Waves from a Binary Neutron Star Inspiral. *Phys. Rev. Lett.* **2017**, *119*, 161101. [[CrossRef](#)]
- Abbott, B.P.; Abbott, R.; Abbott, T.D.; Acernese, F.; Ackley, K.; Adams, C.; Adams, T.; Addesso, P.; Adhikari, R.X.; Adya, V.B.; et al. Multi-messenger Observations of a Binary Neutron Star Merger. *Astrophys. J. Lett.* **2017**, *848*, L12. [[CrossRef](#)]
- Kasliwal, M.M.; Nakar, E.; Singer, L.P.; Kaplan, D.L.; Cook, D.O.; Van Sistine, A.; Lau, R.M.; Fremling, C.; Gottlieb, O.; Jencson, J.E.; et al. Illuminating gravitational waves: A concordant picture of photons from a neutron star merger. *Science* **2017**, *358*, 1559–1565. [[CrossRef](#)]
- Kasen, D.; Metzger, B.; Barnes, J.; Quataert, E.; Ramirez-Ruiz, E. Origin of the heavy elements in binary neutron-star mergers from a gravitational-wave event. *Nature* **2017**, *551*, 80–84. [[CrossRef](#)]
- Smartt, S.J.; Chen, T.W.; Jerkstrand, A.; Coughlin, M.; Kankare, E.; Sim, S.A.; Fraser, M.; Innes, C.; Maguire, K.; Chambers, K.C.; et al. A kilonova as the electromagnetic counterpart to a gravitational-wave source. *Nature* **2017**, *551*, 75–79. [[CrossRef](#)]
- MAGIC Collaboration; Acciari, V.A.; Ansoldi, S.; Antonelli, L.A.; Arbet Engels, A.; Baack, D.; Babić, A.; Banerjee, B.; Barres de Almeida, U.; Barrio, J.A.; et al. Teraelectronvolt emission from the γ -ray burst GRB 190114C. *Nature* **2019**, *575*, 455–458. [[CrossRef](#)]
- Abdalla, H.; Adam, R.; Aharonian, F.; Ait Benkhali, F.; Angüner, E.O.; Arakawa, M.; Arcaro, C.; Armand, C.; Ashkar, H.; Backes, M.; et al. A very-high-energy component deep in the γ -ray burst afterglow. *Nature* **2019**, *575*, 464–467. [[CrossRef](#)]
- Deoskar, K.; Coppin, P.; Friedman, E. Searches for Neutrinos from Precursors and Afterglows of Gamma-ray Bursts using the IceCube Neutrino Observatory. *arXiv* **2021**, arXiv:2107.08870.
- Klebesadel, R.W.; Strong, I.B.; Olson, R.A. Observations of Gamma-Ray Bursts of Cosmic Origin. *Astrophys. J.* **1973**, *182*, L85. [[CrossRef](#)]
- Meegan, C.A.; Fishman, G.J.; Wilson, R.B.; Paciesas, W.S.; Pendleton, G.N.; Horack, J.M.; Brock, M.N.; Kouveliotou, C. Spatial distribution of γ -ray bursts observed by BATSE. *Nature* **1992**, *355*, 143–145. [[CrossRef](#)]
- Band, D.; Matteson, J.; Ford, L.; Schaefer, B.; Palmer, D.; Teegarden, B.; Cline, T.; Briggs, M.; Paciesas, W.; Pendleton, G.; et al. BATSE Observations of Gamma-Ray Burst Spectra. I. Spectral Diversity. *Astrophys. J.* **1993**, *413*, 281. [[CrossRef](#)]
- Abdo, A.A.; Ackermann, M.; Arimoto, M.; Asano, K.; Atwood, W.B.; Axelsson, M.; Baldini, L.; Ballet, J.; Band, D.L.; Barbiellini, G.; et al. Fermi Observations of High-Energy Gamma-Ray Emission from GRB 080916C. *Science* **2009**, *323*, 1688–1693. [[CrossRef](#)]
- Zhang, B. Gamma-Ray Burst Prompt Emission. *Int. J. Mod. Phys. D* **2014**, *23*, 30002. [[CrossRef](#)]
- Kumar, P.; Zhang, B. The physics of gamma-ray bursts and relativistic jets. *Phys. Rep.* **2015**, *561*, 1–109. doi:10.1016/j.physrep.2014.09.008. [[CrossRef](#)]
- Pe’er, A. Physics of Gamma-Ray Bursts Prompt Emission. *Adv. Astron.* **2015**, *2015*, 907321. [[CrossRef](#)]
- Dai, Z.; Daigne, F.; Mészáros, P. The Theory of Gamma-Ray Bursts. *Space Sci. Rev.* **2017**, *212*, 409–427. [[CrossRef](#)]
- Beloborodov, A.M.; Mészáros, P. Photospheric Emission of Gamma-Ray Bursts. *Space Sci. Rev.* **2017**, *207*, 87–110. [[CrossRef](#)]
- Meegan, C.; Lichti, G.; Bhat, P.N.; Bissaldi, E.; Briggs, M.S.; Connaughton, V.; Diehl, R.; Fishman, G.; Greiner, J.; Hoover, A.S.; et al. The Fermi Gamma-ray Burst Monitor. *Astrophys. J.* **2009**, *702*, 791–804. [[CrossRef](#)]
- Poolakkil, S.; Preece, R.; Fletcher, C.; Goldstein, A.; Bhat, P.N.; Bissaldi, E.; Briggs, M.S.; Burns, E.; Cleveland, W.H.; Giles, M.M.; et al. The Fermi GBM Gamma-Ray Burst Spectral Catalog: 10 Years of Data. *arXiv* **2021**, arXiv:2103.13528.
- Goldstein, A.; Burgess, J.M.; Preece, R.D.; Briggs, M.S.; Guiriec, S.; van der Horst, A.e.J.; Connaughton, V.; Wilson-Hodge, C.A.; Paciesas, W.S.; Meegan, C.A.; et al. The Fermi GBM Gamma-Ray Burst Spectral Catalog: The First Two Years. *Astrophys. J. Suppl. Ser.* **2012**, *199*, 19. [[CrossRef](#)]
- Gruber, D.; Goldstein, A.; Weller von Ahlefeld, V.; Narayana Bhat, P.; Bissaldi, E.; Briggs, M.S.; Byrne, D.; Cleveland, W.H.; Connaughton, V.; Diehl, R.; et al. The Fermi GBM Gamma-Ray Burst Spectral Catalog: Four Years of Data. *Astrophys. J. Suppl. Ser.* **2014**, *211*, 12. [[CrossRef](#)]
- Yu, H.F.; Preece, R.D.; Greiner, J.; Narayana Bhat, P.; Bissaldi, E.; Briggs, M.S.; Cleveland, W.H.; Connaughton, V.; Goldstein, A.; von Kienlin, A.; et al. The Fermi GBM gamma-ray burst time-resolved spectral catalog: Brightest bursts in the first four years. *Astron. Astrophys.* **2016**, *588*, A135. [[CrossRef](#)]
- Oganesyan, G.; Nava, L.; Ghirlanda, G.; Celotti, A. Characterization of gamma-ray burst prompt emission spectra down to soft X-rays. *Astron. Astrophys.* **2018**, *616*, A138. [[CrossRef](#)]
- Toffano, M.; Ghirlanda, G.; Nava, L.; Ghisellini, G.; Rasio, M.E.; Oganesyan, G. The slope of the low-energy spectrum of prompt gamma-ray burst emission. *Astron. Astrophys.* **2021**, *652*, A123. [[CrossRef](#)]
- Yu, H.F.; van Eerten, H.J.; Greiner, J.; Sari, R.; Narayana Bhat, P.; von Kienlin, A.; Paciesas, W.S.; Preece, R.D. The sharpness of gamma-ray burst prompt emission spectra. *Astron. Astrophys.* **2015**, *583*, A129. [[CrossRef](#)]
- Acuner, Z.; Ryde, F.; Pe’er, A.; Mortlock, D.; Ahlgren, B. The Fraction of Gamma-Ray Bursts with an Observed Photospheric Emission Episode. *Astrophys. J.* **2020**, *893*, 128. [[CrossRef](#)]
- Daigne, F.; Mochkovitch, R. The expected thermal precursors of gamma-ray bursts in the internal shock model. *Mon. Not. R. Astron. Soc.* **2002**, *336*, 1271–1280. [[CrossRef](#)]

28. Hascoët, R.; Daigne, F.; Mochkovitch, R. Prompt thermal emission in gamma-ray bursts. *Astron. Astrophys.* **2013**, *551*, A124. [[CrossRef](#)]
29. Ghirlanda, G.; Celotti, A.; Ghisellini, G. Extremely hard GRB spectra prune down the forest of emission models. *Astron. Astrophys.* **2003**, *406*, 879–892. [[CrossRef](#)]
30. Acuner, Z.; Ryde, F.; Yu, H.F. Non-dissipative photospheres in GRBs: Spectral appearance in the Fermi/GBM catalogue. *Mon. Not. R. Astron. Soc.* **2019**, *487*, 5508–5519. [[CrossRef](#)]
31. Bosnjak, Z.; Celotti, A.; Ghirlanda, G. GRB 990413: Insight into the thermal phase evolution. *Mon. Not. R. Astron. Soc.* **2006**, *370*, L33–L37. [[CrossRef](#)]
32. Ryde, F.; Pe’er, A. Quasi-blackbody Component and Radiative Efficiency of the Prompt Emission of Gamma-ray Bursts. *Astrophys. J.* **2009**, *702*, 1211–1229. [[CrossRef](#)]
33. Ryde, F.; Pe’er, A.; Nymark, T.; Axelsson, M.; Moretti, E.; Lundman, C.; Battelino, M.; Bissaldi, E.; Chiang, J.; Jackson, M.S.; et al. Observational evidence of dissipative photospheres in gamma-ray bursts. *Mon. Not. R. Astron. Soc.* **2011**, *415*, 3693–3705. [[CrossRef](#)]
34. Guiriec, S.; Mochkovitch, R.; Piran, T.; Daigne, F.; Kouveliotou, C.; Racusin, J.; Gehrels, N.; McEnery, J. GRB 131014A: A Laboratory for Studying the Thermal-like and Non-thermal Emissions in Gamma-Ray Bursts, and the New L^{nTh}_i - $E^{nTh,rest}_{peak,i}$ Relation. *Astrophys. J.* **2015**, *814*, 10. [[CrossRef](#)]
35. Guiriec, S.; Gehrels, N.; McEnery, J.; Kouveliotou, C.; Hartmann, D.H. Photospheric Emission in the Joint GBM and Konus Prompt Spectra of GRB 120323A. *Astrophys. J.* **2017**, *846*, 138. [[CrossRef](#)]
36. Li, L. Thermal Components in Gamma-Ray Bursts. I. How Do They Affect Nonthermal Spectral Parameters? *Astrophys. J. Suppl. Ser.* **2019**, *245*, 7. [[CrossRef](#)]
37. Li, L.; Ryde, F.; Pe’er, A.; Yu, H.F.; Acuner, Z. Bayesian Time-resolved Spectroscopy of Multipulse GRBs: Variations of Emission Properties among Pulses. *Astrophys. J. Suppl. Ser.* **2021**, *254*, 35. [[CrossRef](#)]
38. Kanbach, G.; Bertsch, D.L.; Fichtel, C.E.; Hartman, R.C.; Hunter, S.D.; Kniffen, D.A.; Hughlock, B.W.; Favale, A.; Hofstadter, R.; Hughes, E.B. The project EGRET (energetic gamma-ray experiment telescope) on NASA’s Gamma-Ray Observatory GRO. *Space Sci. Rev.* **1989**, *49*, 69–84. [[CrossRef](#)]
39. Schneid, E.J.; Bertsch, D.L.; Fichtel, C.E.; Hartman, R.C.; Hunter, S.D.; Kanbach, G.; Kniffen, D.A.; Kwok, P.W.; Lin, Y.C.; Mattox, J.R.; et al. EGRET detection of high energy gamma rays from the gamma-ray burst of 3 May 1991. *Astron. Astrophys.* **1992**, *255*, L13.
40. Sommer, M.; Bertsch, D.L.; Dingus, B.L.; Fichtel, C.E.; Fishman, G.J.; Harding, A.K.; Hartman, R.C.; Hunter, S.D.; Hurley, K.; Kanbach, G.; et al. High-Energy Gamma Rays from the Intense 1993 January 31 Gamma-Ray Burst. *Astrophys. J.* **1994**, *422*, L63. [[CrossRef](#)]
41. Hurley, K.; Dingus, B.L.; Mukherjee, R.; Sreekumar, P.; Kouveliotou, C.; Meegan, C.; Fishman, G.J.; Band, D.; Ford, L.; Bertsch, D.; et al. Detection of a γ -ray burst of very long duration and very high energy. *Nature* **1994**, *372*, 652–654. [[CrossRef](#)]
42. González, M.M.; Dingus, B.L.; Kaneko, Y.; Preece, R.D.; Dermer, C.D.; Briggs, M.S. A γ -ray burst with a high-energy spectral component inconsistent with the synchrotron shock model. *Nature* **2003**, *424*, 749–751. [[CrossRef](#)] [[PubMed](#)]
43. Atwood, W.B.; Abdo, A.A.; Ackermann, M.; Althouse, W.; Anderson, B.; Axelsson, M.; Baldini, L.; Ballet, J.; Band, D.L.; Barbiellini, G.; et al. The Large Area Telescope on the Fermi Gamma-Ray Space Telescope Mission. *Astrophys. J.* **2009**, *697*, 1071–1102. [[CrossRef](#)]
44. Ajello, M.; Arimoto, M.; Axelsson, M.; Baldini, L.; Barbiellini, G.; Bastieri, D.; Bellazzini, R.; Bhat, P.N.; Bissaldi, E.; Blandford, R.D.; et al. A Decade of Gamma-Ray Bursts Observed by Fermi-LAT: The Second GRB Catalog. *Astrophys. J.* **2019**, *878*, 52. [[CrossRef](#)]
45. MAGIC Collaboration; Acciari, V.A.; Ansoldi, S.; Antonelli, L.A.; Engels, A.A.; Baack, D.; Babić, A.; Banerjee, B.; Barres de Almeida, U.; Barrio, J.A.; et al. Observation of inverse Compton emission from a long γ -ray burst. *Nature* **2019**, *575*, 459–463. [[CrossRef](#)]
46. Sari, R.; Piran, T. Variability in Gamma-Ray Bursts: A Clue. *Astrophys. J.* **1997**, *485*, 270–273. [[CrossRef](#)]
47. Narayan, R.; Kumar, P. A turbulent model of gamma-ray burst variability. *Mon. Not. R. Astron. Soc.* **2009**, *394*, L117–L120. [[CrossRef](#)]
48. Kouveliotou, C.; Meegan, C.A.; Fishman, G.J.; Bhat, N.P.; Briggs, M.S.; Koshut, T.M.; Paciesas, W.S.; Pendleton, G.N. Identification of two classes of gamma-ray bursts. *Astrophys. J.* **1993**, *413*, L101–L104. [[CrossRef](#)]
49. Bromberg, O.; Nakar, E.; Piran, T.; Sari, R. Short versus Long and Collapsars versus Non-collapsars: A Quantitative Classification of Gamma-Ray Bursts. *Astrophys. J.* **2013**, *764*, 179. [[CrossRef](#)]
50. Ahumada, T.; Singer, L.P.; Anand, S.; Coughlin, M.W.; Kasliwal, M.M.; Ryan, G.; Andreoni, I.; Cenko, S.B.; Fremling, C.; Kumar, H.; et al. Discovery and confirmation of the shortest gamma-ray burst from a collapsar. *Nat. Astron.* **2021**, *5*, 917–927. [[CrossRef](#)]
51. Woosley, S.E. Gamma-ray bursts from stellar mass accretion disks around black holes. *Astrophys. J.* **1993**, *405*, 273–277. [[CrossRef](#)]
52. MacFadyen, A.I.; Woosley, S.E. Collapsars: Gamma-Ray Bursts and Explosions in “Failed Supernovae”. *Astrophys. J.* **1999**, *524*, 262–289. [[CrossRef](#)]
53. Hjorth, J.; Sollerman, J.; Møller, P.; Fynbo, J.P.U.; Woosley, S.E.; Kouveliotou, C.; Tanvir, N.R.; Greiner, J.; Andersen, M.I.; Castro-Tirado, A.J.; et al. A very energetic supernova associated with the γ -ray burst of 29 March 2003. *Nature* **2003**, *423*, 847–850. [[CrossRef](#)]

54. Campana, S.; Mangano, V.; Blustin, A.J.; Brown, P.; Burrows, D.N.; Chincarini, G.; Cummings, J.R.; Cusumano, G.; Della Valle, M.; Malesani, D.; et al. The association of GRB 060218 with a supernova and the evolution of the shock wave. *Nature* **2006**, *442*, 1008–1010. [[CrossRef](#)] [[PubMed](#)]
55. Eichler, D.; Livio, M.; Piran, T.; Schramm, D.N. Nucleosynthesis, neutrino bursts and gamma-rays from coalescing neutron stars. *Nature* **1989**, *340*, 126–128. [[CrossRef](#)]
56. Norris, J.P.; Bonnell, J.T. Short Gamma-Ray Bursts with Extended Emission. *Astrophys. J.* **2006**, *643*, 266–275. [[CrossRef](#)]
57. Genet, F.; Butler, N.R.; Granot, J. The long rapid decay phase of the extended emission from the short GRB 080503. *Mon. Not. R. Astron. Soc.* **2010**, *405*, 695–700. [[CrossRef](#)]
58. Perley, D.A.; Metzger, B.D.; Granot, J.; Butler, N.R.; Sakamoto, T.; Ramirez-Ruiz, E.; Levan, A.J.; Bloom, J.S.; Miller, A.A.; Bunker, A.; et al. GRB 080503: Implications of a Naked Short Gamma-Ray Burst Dominated by Extended Emission. *Astrophys. J.* **2009**, *696*, 1871–1885. [[CrossRef](#)]
59. Bhat, P.N.; Fishman, G.J.; Meegan, C.A.; Wilson, R.B.; Brock, M.N.; Pacieras, W.S. Evidence for sub-millisecond structure in a γ -ray burst. *Nature* **1992**, *359*, 217–218. [[CrossRef](#)]
60. Walker, K.C.; Schaefer, B.E.; Fenimore, E.E. Gamma-Ray Bursts Have Millisecond Variability. *Astrophys. J.* **2000**, *537*, 264–269. [[CrossRef](#)]
61. Piran, T. Gamma-ray bursts and the fireball model. *Phys. Rep.* **1999**, *314*, 575–667. [[CrossRef](#)]
62. Tang, Q.W.; Wang, X.Y.; Liu, R.Y. Evidence of an Internal Dissipation Origin for the High-energy Prompt Emission of GRB 170214A. *Astrophys. J.* **2017**, *844*, 56. [[CrossRef](#)]
63. Rybicki, G.B.; Lightman, A.P. *Radiative Processes in Astrophysics*; Wiley-Interscience: New York, NY, USA, 1979; p. 393.
64. Covino, S.; Lazzati, D.; Ghisellini, G.; Saracco, P.; Campana, S.; Chincarini, G.; di Serego, S.; Cimatti, A.; Vanzi, L.; Pasquini, L.; et al. GRB 990510: Linearly polarized radiation from a fireball. *Astron. Astrophys.* **1999**, *348*, L1–L4.
65. Wijers, R.A.M.J.; Vreeswijk, P.M.; Galama, T.J.; Rol, E.; van Paradijs, J.; Kouveliotou, C.; Giblin, T.; Masetti, N.; Palazzi, E.; Pian, E.; et al. Detection of Polarization in the Afterglow of GRB 990510 with the ESO Very Large Telescope. *Astrophys. J.* **1999**, *523*, L33–L36. [[CrossRef](#)]
66. Gill, R.; Granot, J.; Kumar, P. Linear polarization in gamma-ray burst prompt emission. *MNRAS* **2020**, *491*, 3343–3373. [[CrossRef](#)]
67. Coburn, W.; Boggs, S.E. Polarization of the prompt γ -ray emission from the γ -ray burst of 6 December 2002. *Nature* **2003**, *423*, 415–417. [[CrossRef](#)]
68. Willis, D.R.; Barlow, E.J.; Bird, A.J.; Clark, D.J.; Dean, A.J.; McConnell, M.L.; Moran, L.; Shaw, S.E.; Sguera, V. Evidence of polarisation in the prompt gamma-ray emission from GRB 930131 and GRB 960924. *Astron. Astrophys.* **2005**, *439*, 245–253. [[CrossRef](#)]
69. Kalemci, E.; Boggs, S.E.; Kouveliotou, C.; Finger, M.; Baring, M.G. Search for Polarization from the Prompt Gamma-Ray Emission of GRB 041219a with SPI on INTEGRAL. *Astrophys. J. Suppl. Ser.* **2007**, *169*, 75–82. [[CrossRef](#)]
70. McGlynn, S.; Clark, D.J.; Dean, A.J.; Hanlon, L.; McBreen, S.; Willis, D.R.; McBreen, B.; Bird, A.J.; Foley, S. Polarisation studies of the prompt gamma-ray emission from GRB 041219a using the spectrometer aboard INTEGRAL. *Astron. Astrophys.* **2007**, *466*, 895–904. [[CrossRef](#)]
71. Götz, D.; Laurent, P.; Lebrun, F.; Daigne, F.; Bošnjak, Ž. Variable Polarization Measured in the Prompt Emission of GRB 041219A Using IBIS on Board INTEGRAL. *Astrophys. J.* **2009**, *695*, L208–L212. [[CrossRef](#)]
72. Götz, D.; Covino, S.; Fernández-Soto, A.; Laurent, P.; Bošnjak, Ž. The polarized gamma-ray burst GRB 061122. *Mon. Not. R. Astron. Soc.* **2013**, *431*, 3550–3556. [[CrossRef](#)]
73. Yonetoku, D.; Murakami, T.; Gunji, S.; Mihara, T.; Toma, K.; Sakashita, T.; Morihara, Y.; Takahashi, T.; Toukairin, N.; Fujimoto, H.; et al. Detection of Gamma-Ray Polarization in Prompt Emission of GRB 100826A. *Astrophys. J.* **2011**, *743*, L30. [[CrossRef](#)]
74. Yonetoku, D.; Murakami, T.; Gunji, S.; Mihara, T.; Toma, K.; Morihara, Y.; Takahashi, T.; Wakashima, Y.; Yonemochi, H.; Sakashita, T.; et al. Magnetic Structures in Gamma-Ray Burst Jets Probed by Gamma-Ray Polarization. *Astrophys. J.* **2012**, *758*, L1. [[CrossRef](#)]
75. Rao, A.R.; Chand, V.; Hingar, M.K.; Iyyani, S.; Khanna, R.; Kutty, A.P.K.; Malkar, J.P.; Paul, D.; Bhalerao, V.B.; Bhattacharya, D.; et al. AstroSat CZT Imager Observations of GRB 151006A: Timing, Spectroscopy, and Polarization Study. *Astrophys. J.* **2016**, *833*, 86. [[CrossRef](#)]
76. Chand, V.; Chattopadhyay, T.; Oganessian, G.; Rao, A.R.; Vadawale, S.V.; Bhattacharya, D.; Bhalerao, V.B.; Misra, K. AstroSat-CZTI Detection of Variable Prompt Emission Polarization in GRB 171010A. *Astrophys. J.* **2019**, *874*, 70. [[CrossRef](#)]
77. Sharma, V.; Iyyani, S.; Bhattacharya, D.; Chattopadhyay, T.; Rao, A.R.; Aarthy, E.; Vadawale, S.V.; Mithun, N.P.S.; Bhalerao, V.B.; Ryde, F.; et al. Time-varying Polarized Gamma-Rays from GRB 160821A: Evidence for Ordered Magnetic Fields. *Astrophys. J.* **2019**, *882*, L10. [[CrossRef](#)]
78. Kole, M.; De Angelis, N.; Berlato, F.; Burgess, J.M.; Gauvin, N.; Greiner, J.; Hajdas, W.; Li, H.C.; Li, Z.H.; Produit, N.; et al. The POLAR Gamma-Ray Burst Polarization Catalog. *arXiv* **2020**, arXiv:2009.04871.
79. Mészáros, P.; Rees, M.J.; Papathanassiou, H. Spectral properties of blast-wave models of gamma-ray burst sources. *Astrophys. J.* **1994**, *432*, 181–193. [[CrossRef](#)]
80. Daigne, F.; Mochkovitch, R. The physics of pulses in gamma-ray bursts: Emission processes, temporal profiles and time-lags. *Mon. Not. R. Astron. Soc.* **2003**, *342*, 587–592. [[CrossRef](#)]
81. Thompson, C. A Model of Gamma-Ray Bursts. *Mon. Not. R. Astron. Soc.* **1994**, *270*, 480–498. [[CrossRef](#)]

82. Rees, M.J.; Mészáros, P. Dissipative Photosphere Models of Gamma-Ray Bursts and X-Ray Flashes. *Astrophys. J.* **2005**, *628*, 847–852. [[CrossRef](#)]
83. Pe’er, A. Temporal Evolution of Thermal Emission from Relativistically Expanding Plasma. *Astrophys. J.* **2008**, *682*, 463–473. [[CrossRef](#)]
84. Toma, K.; Wu, X.F.; Mészáros, P. Photosphere-internal shock model of gamma-ray bursts: Case studies of Fermi/LAT bursts. *Mon. Not. R. Astron. Soc.* **2011**, *415*, 1663–1680. [[CrossRef](#)]
85. Cavallo, G.; Rees, M.J. A qualitative study of cosmic fireballs and γ -ray bursts. *Mon. Not. R. Astron. Soc.* **1978**, *183*, 359–365. [[CrossRef](#)]
86. Paczynski, B. Gamma-ray bursters at cosmological distances. *Astrophys. J.* **1986**, *308*, L43–L46. [[CrossRef](#)]
87. Goodman, J. Are gamma-ray bursts optically thick? *Astrophys. J.* **1986**, *308*, L47–L50. [[CrossRef](#)]
88. Shemi, A.; Piran, T. The Appearance of Cosmic Fireballs. *Astrophys. J.* **1990**, *365*, L55. [[CrossRef](#)]
89. Meszaros, P.; Rees, M.J. Relativistic fireballs and their impact on external matter—Models for cosmological gamma-ray bursts. *Astrophys. J.* **1993**, *405*, 278–284. [[CrossRef](#)]
90. Mészáros, P.; Rees, M.J. Steep Slopes and Preferred Breaks in Gamma-Ray Burst Spectra: The Role of Photospheres and Comptonization. *Astrophys. J.* **2000**, *530*, 292–298. [[CrossRef](#)]
91. Mészáros, P.; Ramirez-Ruiz, E.; Rees, M.J.; Zhang, B. X-Ray-rich Gamma-Ray Bursts, Photospheres, and Variability. *Astrophys. J.* **2002**, *578*, 812–817. [[CrossRef](#)]
92. Beloborodov, A.M. Collisional mechanism for gamma-ray burst emission. *Mon. Not. R. Astron. Soc.* **2010**, *407*, 1033–1047. [[CrossRef](#)]
93. Pe’er, A.; Ryde, F. A Theory of Multicolor Blackbody Emission from Relativistically Expanding Plasmas. *Astrophys. J.* **2011**, *732*, 49. [[CrossRef](#)]
94. Deng, W.; Zhang, B. Low Energy Spectral Index and E_p Evolution of Quasi-thermal Photosphere Emission of Gamma-Ray Bursts. *Astrophys. J.* **2014**, *785*, 112. [[CrossRef](#)]
95. Lundman, C.; Pe’er, A.; Ryde, F. A theory of photospheric emission from relativistic, collimated outflows. *Mon. Not. R. Astron. Soc.* **2013**, *428*, 2430–2442. [[CrossRef](#)]
96. Abdo, A.A.; Ackermann, M.; Ajello, M.; Asano, K.; Atwood, W.B.; Axelsson, M.; Baldini, L.; Ballet, J.; Barbiellini, G.; Baring, M.G.; et al. Fermi Observations of GRB 090902B: A Distinct Spectral Component in the Prompt and Delayed Emission. *Astrophys. J.* **2009**, *706*, L138–L144. [[CrossRef](#)]
97. Zhang, B.; Pe’er, A. Evidence of an Initially Magnetically Dominated Outflow in GRB 080916C. *Astrophys. J.* **2009**, *700*, L65–L68. [[CrossRef](#)]
98. Wijers, R.A.M.J.; Rees, M.J.; Meszaros, P. Shocked by GRB 970228: The afterglow of a cosmological fireball. *Mon. Not. R. Astron. Soc.* **1997**, *288*, L51–L56. [[CrossRef](#)]
99. Sari, R.; Piran, T.; Narayan, R. Spectra and Light Curves of Gamma-Ray Burst Afterglows. *Astrophys. J.* **1998**, *497*, L17–L20. [[CrossRef](#)]
100. Fermi, E. On the Origin of the Cosmic Radiation. *Phys. Rev.* **1949**, *75*, 1169–1174. [[CrossRef](#)]
101. Fermi, E. Galactic Magnetic Fields and the Origin of Cosmic Radiation. *Astrophys. J.* **1954**, *119*, 1. [[CrossRef](#)]
102. Bell, A.R. The acceleration of cosmic rays in shock fronts. I. *Mon. Not. R. Astron. Soc.* **1978**, *182*, 147–156. [[CrossRef](#)]
103. Blandford, R.D.; Ostriker, J.P. Particle acceleration by astrophysical shocks. *Astrophys. J.* **1978**, *221*, L29–L32. [[CrossRef](#)]
104. Blandford, R.; Eichler, D. Particle acceleration at astrophysical shocks: A theory of cosmic ray origin. *Phys. Rep.* **1987**, *154*, 1–75. [[CrossRef](#)]
105. Jones, F.C.; Ellison, D.C. The plasma physics of shock acceleration. *Space Sci. Rev.* **1991**, *58*, 259–346. [[CrossRef](#)]
106. Silva, L.O.; Fonseca, R.A.; Tonge, J.W.; Dawson, J.M.; Mori, W.B.; Medvedev, M.V. Interpenetrating Plasma Shells: Near-equipartition Magnetic Field Generation and Nonthermal Particle Acceleration. *Astrophys. J.* **2003**, *596*, L121–L124. [[CrossRef](#)]
107. Nishikawa, K.I.; Hardee, P.; Richardson, G.; Preece, R.; Sol, H.; Fishman, G.J. Particle Acceleration in Relativistic Jets Due to Weibel Instability. *Astrophys. J.* **2003**, *595*, 555–563. [[CrossRef](#)]
108. Spitkovsky, A. Particle Acceleration in Relativistic Collisionless Shocks: Fermi Process at Last? *Astrophys. J.* **2008**, *682*, L5. [[CrossRef](#)]
109. Haugbølle, T. Three-dimensional Modeling of Relativistic Collisionless Ion-electron Shocks. *Astrophys. J.* **2011**, *739*, L42. [[CrossRef](#)]
110. Sironi, L.; Spitkovsky, A. Particle Acceleration in Relativistic Magnetized Collisionless Pair Shocks: Dependence of Shock Acceleration on Magnetic Obliquity. *Astrophys. J.* **2009**, *698*, 1523–1549. [[CrossRef](#)]
111. Sironi, L.; Spitkovsky, A. Particle Acceleration in Relativistic Magnetized Collisionless Electron-Ion Shocks. *Astrophys. J.* **2011**, *726*, 75. [[CrossRef](#)]
112. Summerlin, E.J.; Baring, M.G. Diffusive Acceleration of Particles at Oblique, Relativistic, Magnetohydrodynamic Shocks. *Astrophys. J.* **2012**, *745*, 63. [[CrossRef](#)]
113. Sironi, L.; Spitkovsky, A. Relativistic Reconnection: An Efficient Source of Non-thermal Particles. *Astrophys. J.* **2014**, *783*, L21. [[CrossRef](#)]
114. Lemoine, M.; Vanthieghem, A.; Pelletier, G.; Gremillet, L. Physics of relativistic collisionless shocks. II. Dynamics of the background plasma. *Phys. Rev. E* **2019**, *100*, 033209. [[CrossRef](#)] [[PubMed](#)]

115. Nagar, Y.; Keshet, U. Diffusive acceleration in relativistic shocks: Particle feedback. *Mon. Not. R. Astron. Soc.* **2021**, *501*, 329–336. [[CrossRef](#)]
116. Kundu, S.; Vaidya, B.; Mignone, A. Numerical Modeling and Physical Interplay of Stochastic Turbulent Acceleration for Nonthermal Emission Processes. *Astrophys. J.* **2021**, *921*, 74. [[CrossRef](#)]
117. Sironi, L.; Petropoulou, M.; Giannios, D. Relativistic jets shine through shocks or magnetic reconnection? *Mon. Not. R. Astron. Soc.* **2015**, *450*, 183–191. [[CrossRef](#)]
118. Zenitani, S.; Hoshino, M. The Generation of Nonthermal Particles in the Relativistic Magnetic Reconnection of Pair Plasmas. *Astrophys. J.* **2001**, *562*, L63–L66. [[CrossRef](#)]
119. Zenitani, S.; Hoshino, M. Particle Acceleration and Magnetic Dissipation in Relativistic Current Sheet of Pair Plasmas. *Astrophys. J.* **2007**, *670*, 702–726. [[CrossRef](#)]
120. McKinney, J.C.; Uzdensky, D.A. A reconnection switch to trigger gamma-ray burst jet dissipation. *Mon. Not. R. Astron. Soc.* **2012**, *419*, 573–607. [[CrossRef](#)]
121. Guo, F.; Li, H.; Daughton, W.; Liu, Y.H. Formation of Hard Power Laws in the Energetic Particle Spectra Resulting from Relativistic Magnetic Reconnection. *Phys. Rev. Lett.* **2014**, *113*, 155005. [[CrossRef](#)]
122. Guo, F.; Liu, Y.H.; Daughton, W.; Li, H. Particle Acceleration and Plasma Dynamics during Magnetic Reconnection in the Magnetically Dominated Regime. *Astrophys. J.* **2015**, *806*, 167. [[CrossRef](#)]
123. Sironi, L.; Giannios, D.; Petropoulou, M. Plasmoids in relativistic reconnection, from birth to adulthood: First they grow, then they go. *Mon. Not. R. Astron. Soc.* **2016**, *462*, 48–74. [[CrossRef](#)]
124. Werner, G.R.; Uzdensky, D.A. Nonthermal Particle Acceleration in 3D Relativistic Magnetic Reconnection in Pair Plasma. *Astrophys. J.* **2017**, *843*, L27. [[CrossRef](#)]
125. Kagan, D.; Nakar, E.; Piran, T. Physics of the saturation of particle acceleration in relativistic magnetic reconnection. *Mon. Not. R. Astron. Soc.* **2018**, *476*, 3902–3912. [[CrossRef](#)]
126. Rees, M.J.; Meszaros, P. Unsteady outflow models for cosmological gamma-ray bursts. *Astrophys. J.* **1994**, *430*, L93–L96. [[CrossRef](#)]
127. Paczynski, B.; Xu, G. Neutrino bursts from gamma-ray bursts. *Astrophys. J.* **1994**, *427*, 708–713. [[CrossRef](#)]
128. Kobayashi, S.; Piran, T.; Sari, R. Can Internal Shocks Produce the Variability in Gamma-Ray Bursts? *Astrophys. J.* **1997**, *490*, 92. [[CrossRef](#)]
129. Daigne, F.; Mochkovitch, R. Gamma-ray bursts from internal shocks in a relativistic wind: Temporal and spectral properties. *Mon. Not. R. Astron. Soc.* **1998**, *296*, 275–286. [[CrossRef](#)]
130. Kumar, P.; McMahon, E. A general scheme for modelling γ -ray burst prompt emission. *Mon. Not. R. Astron. Soc.* **2008**, *384*, 33–63. [[CrossRef](#)]
131. Bošnjak, Ž.; Daigne, F.; Dubus, G. Prompt high-energy emission from γ -ray bursts in the internal shock model. *Astron. Astrophys.* **2009**, *498*, 677–703. [[CrossRef](#)]
132. Bošnjak, Ž.; Daigne, F. Spectral evolution in gamma-ray bursts: Predictions of the internal shock model and comparison to observations. *Astron. Astrophys.* **2014**, *568*, A45. [[CrossRef](#)]
133. Daigne, F.; Mochkovitch, R. Gamma-ray bursts from internal shocks in a relativistic wind: A hydrodynamical study. *Astron. Astrophys.* **2000**, *358*, 1157–1166.
134. Mimica, P.; Aloy, M.A.; Müller, E. Internal shocks in relativistic outflows: Collisions of magnetized shells. *Astron. Astrophys.* **2007**, *466*, 93–106. [[CrossRef](#)]
135. Sari, R.; Piran, T. Cosmological gamma-ray bursts: Internal versus external shocks. *Mon. Not. R. Astron. Soc.* **1997**, *287*, 110–116. [[CrossRef](#)]
136. Kumar, P. Gamma-Ray Burst Energetics. *Astrophys. J.* **1999**, *523*, L113–L116. [[CrossRef](#)]
137. Spada, M.; Panaitescu, A.; Mészáros, P. Analysis of Temporal Features of Gamma-Ray Bursts in the Internal Shock Model. *Astrophys. J.* **2000**, *537*, 824–832. [[CrossRef](#)]
138. Lloyd, N.M.; Petrosian, V. Synchrotron Radiation as the Source of Gamma-Ray Burst Spectra. *Astrophys. J.* **2000**, *543*, 722–732. [[CrossRef](#)]
139. Bykov, A.M.; Meszaros, P. Electron Acceleration and Efficiency in Nonthermal Gamma-Ray Sources. *Astrophys. J.* **1996**, *461*, L37. [[CrossRef](#)]
140. Spruit, H.C.; Daigne, F.; Drenkhahn, G. Large scale magnetic fields and their dissipation in GRB fireballs. *Astron. Astrophys.* **2001**, *369*, 694–705. [[CrossRef](#)]
141. Gruzinov, A.; Mészáros, P. Photon Acceleration in Variable Ultrarelativistic Outflows and High-Energy Spectra of Gamma-Ray Bursts. *Astrophys. J.* **2000**, *539*, L21–L24. [[CrossRef](#)]
142. Kumar, P.; Narayan, R. GRB 080319B: Evidence for relativistic turbulence, not internal shocks. *Mon. Not. R. Astron. Soc.* **2009**, *395*, 472–489. [[CrossRef](#)]
143. Zou, Y.C.; Piran, T.; Sari, R. Clues from the Prompt Emission of GRB 080319B. *Astrophys. J.* **2009**, *692*, L92–L95. [[CrossRef](#)]
144. Derishev, E.V.; Kocharovskiy, V.V.; Kocharovskiy, V.V. The Neutron Component in Fireballs of Gamma-Ray Bursts: Dynamics and Observable Imprints. *Astrophys. J.* **1999**, *521*, 640–649. [[CrossRef](#)]
145. Mészáros, P.; Rees, M.J. Multi-GEV Neutrinos from Internal Dissipation in Gamma-Ray Burst Fireballs. *Astrophys. J.* **2000**, *541*, L5–L8. [[CrossRef](#)]
146. Beloborodov, A.M. Nuclear Composition of Gamma-Ray Burst Fireballs. *Astrophys. J.* **2003**, *588*, 931–944. [[CrossRef](#)]

147. Beloborodov, A.M. Hyper-accreting black holes. In *Cool Discs, Hot Flows: The Varying Faces of Accreting Compact Objects*; Axelsson, M., Ed.; American Institute of Physics Conference Series; 2008; Volume 1054, pp. 51–70. Available online: <https://ui.adsabs.harvard.edu/abs/2008AIPC.1054...51B> (accessed on 1 December 2021).
148. Vurm, I.; Beloborodov, A.M.; Poutanen, J. Gamma-Ray Bursts from Magnetized Collisionally Heated Jets. *Astrophys. J.* **2011**, *738*, 77. [[CrossRef](#)]
149. Usov, V.V. Millisecond pulsars with extremely strong magnetic fields as a cosmological source of γ -ray bursts. *Nature* **1992**, *357*, 472–474. [[CrossRef](#)]
150. Mészáros, P.; Rees, M.J. Poynting Jets from Black Holes and Cosmological Gamma-Ray Bursts. *Astrophys. J.* **1997**, *482*, L29–L32. [[CrossRef](#)]
151. Spruit, H.C. Gamma-ray bursts from X-ray binaries. *Astron. Astrophys.* **1999**, *341*, L1–L4.
152. Lyutikov, M.; Blandford, R. Gamma Ray Bursts as Electromagnetic Outflows. *arXiv* **2003**, arXiv:astro-ph/0312347.
153. Narayan, R.; Kumar, P.; Tchekhovskoy, A. Constraints on cold magnetized shocks in gamma-ray bursts. *Mon. Not. R. Astron. Soc.* **2011**, *416*, 2193–2201. [[CrossRef](#)]
154. Kumar, P.; Crumley, P. Radiation from a relativistic Poynting jet: Some general considerations. *Mon. Not. R. Astron. Soc.* **2015**, *453*, 1820–1828. [[CrossRef](#)]
155. Drenkhahn, G. Acceleration of GRB outflows by Poynting flux dissipation. *Astron. Astrophys.* **2002**, *387*, 714–724. [[CrossRef](#)]
156. Drenkhahn, G.; Spruit, H.C. Efficient acceleration and radiation in Poynting flux powered GRB outflows. *Astron. Astrophys.* **2002**, *391*, 1141–1153. [[CrossRef](#)]
157. Giannios, D.; Spruit, H.C. Spectra of Poynting-flux powered GRB outflows. *Astron. Astrophys.* **2005**, *430*, 1–7. [[CrossRef](#)]
158. Giannios, D. Prompt GRB emission from gradual energy dissipation. *Astron. Astrophys.* **2008**, *480*, 305–312. [[CrossRef](#)]
159. Bégué, D.; Pe’er, A.; Lyubarsky, Y. Radiative striped wind model for gamma-ray bursts. *Mon. Not. R. Astron. Soc.* **2017**, *467*, 2594–2611. [[CrossRef](#)]
160. Giannios, D.; Uzdensky, D.A. GRB and blazar jets shining through their stripes. *Mon. Not. R. Astron. Soc.* **2019**, *484*, 1378–1389. [[CrossRef](#)]
161. Giannios, D. Prompt emission spectra from the photosphere of a GRB. *Astron. Astrophys.* **2006**, *457*, 763–770. [[CrossRef](#)]
162. Giannios, D. The peak energy of dissipative gamma-ray burst photospheres. *Mon. Not. R. Astron. Soc.* **2012**, *422*, 3092–3098. [[CrossRef](#)]
163. Beniamini, P.; Giannios, D. Prompt gamma-ray burst emission from gradual magnetic dissipation. *MNRAS* **2017**, *468*, 3202–3211. [[CrossRef](#)]
164. Gill, R.; Granot, J.; Beniamini, P. GRB spectrum from gradual dissipation in a magnetized outflow. *Mon. Not. R. Astron. Soc.* **2020**, *499*, 1356–1372. [[CrossRef](#)]
165. Contopoulos, J. A Simple Type of Magnetically Driven Jets: An Astrophysical Plasma Gun. *Astrophys. J.* **1995**, *450*, 616. [[CrossRef](#)]
166. Granot, J.; Komissarov, S.S.; Spitkovsky, A. Impulsive acceleration of strongly magnetized relativistic flows. *Mon. Not. R. Astron. Soc.* **2011**, *411*, 1323–1353. [[CrossRef](#)]
167. Granot, J. The effects of sub-shells in highly magnetized relativistic flows. *Mon. Not. R. Astron. Soc.* **2012**, *421*, 2467–2477. [[CrossRef](#)]
168. Komissarov, S.S. Shock dissipation in magnetically dominated impulsive flows. *Mon. Not. R. Astron. Soc.* **2012**, *422*, 326–346. [[CrossRef](#)]
169. Lazar, A.; Nakar, E.; Piran, T. Gamma-Ray Burst Light Curves in the Relativistic Turbulence and Relativistic Subject Models. *Astrophys. J.* **2009**, *695*, L10–L14. [[CrossRef](#)]
170. Zhang, B.; Yan, H. The Internal-collision-induced Magnetic Reconnection and Turbulence (ICMART) Model of Gamma-ray Bursts. *Astrophys. J.* **2011**, *726*, 90. [[CrossRef](#)]
171. Beniamini, P.; Granot, J. Properties of GRB light curves from magnetic reconnection. *Mon. Not. R. Astron. Soc.* **2016**, *459*, 3635–3658. [[CrossRef](#)]
172. Barniol Duran, R.; Leng, M.; Giannios, D. An anisotropic minijets model for the GRB prompt emission. *Mon. Not. R. Astron. Soc.* **2016**, *455*, L6–L10. [[CrossRef](#)]
173. Ackermann, M.; Ajello, M.; Asano, K.; Axelsson, M.; Baldini, L.; Ballet, J.; Barbiellini, G.; Bastieri, D.; Bechtol, K.; Bellazzini, R.; et al. The First Fermi-LAT Gamma-Ray Burst Catalog. *Astrophys. J. Suppl. Ser.* **2013**, *209*, 11. [[CrossRef](#)]
174. Rees, M.J.; Mészáros, P. Relativistic fireballs: Energy conversion and time-scales. *Mon. Not. R. Astron. Soc.* **1992**, *258*, 41P–43P. [[CrossRef](#)]
175. Meszaros, P.; Laguna, P.; Rees, M.J. Gasdynamics of relativistically expanding gamma-ray burst sources—Kinematics, energetics, magnetic fields, and efficiency. *Astrophys. J.* **1993**, *415*, 181–190. [[CrossRef](#)]
176. Papathanassiou, H.; Meszaros, P. Spectra of Unsteady Wind Models of Gamma-Ray Bursts. *Astrophys. J.* **1996**, *471*, L91. [[CrossRef](#)]
177. Beniamini, P.; Piran, T. Constraints on the Synchrotron Emission Mechanism in Gamma-Ray Bursts. *Astrophys. J.* **2013**, *769*, 69. [[CrossRef](#)]
178. Beniamini, P.; Piran, T. The emission mechanism in magnetically dominated gamma-ray burst outflows. *Mon. Not. R. Astron. Soc.* **2014**, *445*, 3892–3907. [[CrossRef](#)]
179. Katz, J.I. Low-frequency spectra of gamma-ray bursts. *Astrophys. J.* **1994**, *432*, L107–L109. [[CrossRef](#)]

180. Pe'er, A.; Zhang, B. Synchrotron Emission in Small-Scale Magnetic Fields as a Possible Explanation for Prompt Emission Spectra of Gamma-Ray Bursts. *Astrophys. J.* **2006**, *653*, 454–461. [[CrossRef](#)]
181. Zhao, X.; Li, Z.; Liu, X.; Zhang, B.B.; Bai, J.; Mészáros, P. Gamma-Ray Burst Spectrum with Decaying Magnetic Field. *Astrophys. J.* **2014**, *780*, 12. [[CrossRef](#)]
182. Bhattacharya, M.; Kumar, P. On explaining prompt emission from GRB central engines with photospheric emission model. *arXiv* **2021**, arXiv:2110.14792.
183. Derishev, E.V. Synchrotron emission in the fast cooling regime: Which spectra can be explained? *Astrophys. Space Sci.* **2007**, *309*, 157–161. [[CrossRef](#)]
184. Nakar, E.; Ando, S.; Sari, R. Klein-Nishina Effects on Optically Thin Synchrotron and Synchrotron Self-Compton Spectrum. *Astrophys. J.* **2009**, *703*, 675–691. [[CrossRef](#)]
185. Daigne, F.; Bošnjak, Ž.; Dubus, G. Reconciling observed gamma-ray burst prompt spectra with synchrotron radiation? *Astron. Astrophys.* **2011**, *526*, A110. [[CrossRef](#)]
186. Barniol Duran, R.; Bošnjak, Ž.; Kumar, P. Inverse-Compton cooling in Klein-Nishina regime and gamma-ray burst prompt spectrum. *Mon. Not. R. Astron. Soc.* **2012**, *424*, 3192–3200. [[CrossRef](#)]
187. Beniamini, P.; Barniol Duran, R.; Giannios, D. Marginally fast cooling synchrotron models for prompt GRBs. *Mon. Not. R. Astron. Soc.* **2018**, *476*, 1785–1795. [[CrossRef](#)]
188. Piran, T.; Sari, R.; Zou, Y.C. Observational limits on inverse Compton processes in gamma-ray bursts. *Mon. Not. R. Astron. Soc.* **2009**, *393*, 1107–1113. [[CrossRef](#)]
189. Paczynski, B. Super-Eddington winds from neutron stars. *Astrophys. J.* **1990**, *363*, 218–226. [[CrossRef](#)]
190. Preece, R.D.; Briggs, M.S.; Mallozzi, R.S.; Pendleton, G.N.; Paciesas, W.S.; Band, D.L. The Synchrotron Shock Model Confronts a “Line of Death” in the BATSE Gamma-Ray Burst Data. *Astrophys. J.* **1998**, *506*, L23–L26. [[CrossRef](#)]
191. Eichler, D.; Levinson, A. A Compact Fireball Model of Gamma-Ray Bursts. *Astrophys. J.* **2000**, *529*, 146–150. [[CrossRef](#)]
192. Pe'er, A.; Waxman, E. Prompt Gamma-Ray Burst Spectra: Detailed Calculations and the Effect of Pair Production. *Astrophys. J.* **2004**, *613*, 448–459. [[CrossRef](#)]
193. Pe'er, A.; Mészáros, P.; Rees, M.J. Peak Energy Clustering and Efficiency in Compact Objects. *Astrophys. J.* **2005**, *635*, 476–480. [[CrossRef](#)]
194. Pe'er, A.; Mészáros, P.; Rees, M.J. The Observable Effects of a Photospheric Component on GRB and XRF Prompt Emission Spectrum. *Astrophys. J.* **2006**, *642*, 995–1003. [[CrossRef](#)]
195. Beloborodov, A.M. Radiative Transfer in Ultrarelativistic Outflows. *Astrophys. J.* **2011**, *737*, 68. [[CrossRef](#)]
196. Vereshchagin, G.V. Physics of Nondissipative Ultrarelativistic Photospheres. *Int. J. Mod. Phys. D* **2014**, *23*, 30003. [[CrossRef](#)]
197. Ito, H.; Nagataki, S.; Ono, M.; Lee, S.H.; Mao, J.; Yamada, S.; Pe'er, A.; Mizuta, A.; Harikae, S. Photospheric Emission from Stratified Jets. *Astrophys. J.* **2013**, *777*, 62. [[CrossRef](#)]
198. Lundman, C.; Pe'er, A.; Ryde, F. Polarization properties of photospheric emission from relativistic, collimated outflows. *Mon. Not. R. Astron. Soc.* **2014**, *440*, 3292–3308. [[CrossRef](#)]
199. Meng, Y.Z.; Liu, L.D.; Wei, J.J.; Wu, X.F.; Zhang, B.B. The Time-resolved Spectra of Photospheric Emission from a Structured Jet for Gamma-Ray Bursts. *Astrophys. J.* **2019**, *882*, 26. [[CrossRef](#)]
200. Parsotan, T.; Lazzati, D. Monte Carlo Simulations of Photospheric Emission in Gamma Ray Bursts. *arXiv* **2021**, arXiv:2110.13038.
201. Eichler, D.; Manis, H. Spectral Lags Explained as Scattering from Accelerated Scatterers. *Astrophys. J.* **2008**, *689*, L85. [[CrossRef](#)]
202. Eichler, D. Cloaked Gamma-Ray Bursts. *Astrophys. J.* **2014**, *787*, L32. [[CrossRef](#)]
203. Vyas, M.K.; Pe'er, A.; Eichler, D. A Backscattering-dominated Prompt Emission Model for the Prompt Phase of Gamma-Ray Bursts. *Astrophys. J.* **2021**, *908*, 9. [[CrossRef](#)]
204. Vyas, M.K.; Pe'er, A.; Eichler, D. Predicting Spectral Parameters in the Backscattering-dominated Model for the Prompt Phase of GRBs. *Astrophys. J.* **2021**, *918*, L12. [[CrossRef](#)]
205. Amati, L.; Frontera, F.; Tavani, M.; in't Zand, J.J.M.; Antonelli, A.; Costa, E.; Feroci, M.; Guidorzi, C.; Heise, J.; Masetti, N.; et al. Intrinsic spectra and energetics of BeppoSAX Gamma-Ray Bursts with known redshifts. *Astron. Astrophys.* **2002**, *390*, 81–89. [[CrossRef](#)]
206. Pe'er, A.; Zhang, B.B.; Ryde, F.; McGlynn, S.; Zhang, B.; Preece, R.D.; Kouveliotou, C. The connection between thermal and non-thermal emission in gamma-ray bursts: General considerations and GRB 090902B as a case study. *Mon. Not. R. Astron. Soc.* **2012**, *420*, 468–482. [[CrossRef](#)]
207. Gupta, N.; Zhang, B. Prompt emission of high-energy photons from gamma ray bursts. *Mon. Not. R. Astron. Soc.* **2007**, *380*, 78–92. [[CrossRef](#)]
208. Fan, Y.Z.; Piran, T. High-energy γ -ray emission from gamma-ray bursts—Before GLAST. *Front. Phys. China* **2008**, *3*, 306–330. [[CrossRef](#)]
209. Asano, K.; Inoue, S.; Mészáros, P. Prompt High-Energy Emission from Proton-Dominated Gamma-Ray Bursts. *Astrophys. J.* **2009**, *699*, 953–957. [[CrossRef](#)]
210. Wang, X.Y.; Li, Z.; Dai, Z.G.; Mészáros, P. GRB 080916C: On the Radiation Origin of the Prompt Emission from keV/MeV TO GeV. *Astrophys. J.* **2009**, *698*, L98–L102. [[CrossRef](#)]

211. Razzaque, S.; Dermer, C.D.; Finke, J.D. Synchrotron Radiation from Ultra-High Energy Protons and the Fermi Observations of GRB 080916C. *Open Astron. J.* **2010**, *3*, 150–155. [[CrossRef](#)]
212. Asano, K.; Mészáros, P. Delayed Onset of High-energy Emissions in Leptonic and Hadronic Models of Gamma-Ray Bursts. *Astrophys. J.* **2012**, *757*, 115. [[CrossRef](#)]
213. Crumley, P.; Kumar, P. Hadronic models for Large Area Telescope prompt emission observed in Fermi gamma-ray bursts. *Mon. Not. R. Astron. Soc.* **2013**, *429*, 3238–3251. [[CrossRef](#)]
214. Ghisellini, G.; Ghirlanda, G.; Oganessian, G.; Ascenzi, S.; Nava, L.; Celotti, A.; Salafia, O.S.; Ravasio, M.E.; Ronchi, M. Proton-synchrotron as the radiation mechanism of the prompt emission of gamma-ray bursts? *Astron. Astrophys.* **2020**, *636*, A82. [[CrossRef](#)]
215. Schüssler, F. The Transient program of the Cherenkov Telescope Array. *arXiv* **2019**, arXiv:1907.07567.
216. Fioretti, V.; Ribeiro, D.; Humensky, T.B.; Bulgarelli, A.; Maier, G.; Moralejo, A.; Nigro, C. The Cherenkov Telescope Array sensitivity to the transient sky. *arXiv* **2019**, arXiv:1907.08018.
217. Inoue, S.; Granot, J.; O'Brien, P.T.; Asano, K.; Bouvier, A.; Carosi, A.; Connaughton, V.; Garczarczyk, M.; Gilmore, R.; Hinton, J.; et al. Gamma-ray burst science in the era of the Cherenkov Telescope Array. *Astropart. Phys.* **2013**, *43*, 252–275. [[CrossRef](#)]
218. Kakuwa, J.; Murase, K.; Toma, K.; Inoue, S.; Yamazaki, R.; Ioka, K. Prospects for detecting gamma-ray bursts at very high energies with the Cherenkov Telescope Array. *Mon. Not. R. Astron. Soc.* **2012**, *425*, 514–526. [[CrossRef](#)]
219. Wei, J.; Cordier, B.; Antier, S.; Antilogus, P.; Atteia, J.L.; Bajat, A.; Basa, S.; Beckmann, V.; Bernardini, M.G.; Boissier, S.; et al. The Deep and Transient Universe in the SVOM Era: New Challenges and Opportunities—Scientific prospects of the SVOM mission. *arXiv* **2016**, arXiv:1610.06892.
220. Rudolph, A.; Bošnjak, Ž.; Palladino, A.; Sadeh, I.; Winter, W. Multi-wavelength radiation models for low-luminosity GRBs, and the implications for UHECRs. *arXiv* **2021**, arXiv:2107.04612.
221. Punturo, M.; Abernathy, M.; Acernese, F.; Allen, B.; Andersson, N.; Arun, K.; Barone, F.; Barr, B.; Barsuglia, M.; Beker, M.; et al. The Einstein Telescope: A third-generation gravitational wave observatory. *Class. Quantum Gravity* **2010**, *27*, 194002. [[CrossRef](#)]
222. Clark, B.A.; IceCube-Gen2 collaboration. The IceCube-Gen2 Neutrino Observatory. *J. Instrum.* **2021**, *16*, C10007. [[CrossRef](#)]
223. Piro, L.; Ahlers, M.; Coleiro, A.; Colpi, M.; de Oña Wilhelmi, E.; Guainazzi, M.; Jonker, P.G.; Mc Namara, P.; Nichols, D.A.; O'Brien, P.; et al. Multi-messenger-Athena Synergy White Paper. *arXiv* **2021**, arXiv:2110.15677.
224. Pitik, T.; Tamborra, I.; Petropoulou, M. Neutrino signal dependence on gamma-ray burst emission mechanism. *J. Cosmol. Astropart. Phys.* **2021**, *2021*, 034. [[CrossRef](#)]